On the use of single, dual and three process langmuir models for binary gas mixtures that exhibit unique combinations of these processes

Kyle J. Tynan[1] · Sofia Tosso[1] · Armin D. Ebner[1] · James A. Ritter[1]

Abstract

Two scenarios were investigated for predicting binary gas adsorption equilibria when the single gas isotherms of one component is described by the three process Langmuir (TPL) model and the single gas isotherms of the other component is described by either the dual process Langmuir (DPL) or single process Langmuir (SPL) model. For the TPL–SPL and TPL–DPL models, 7 and 12 different correlations of energetic (free energy) site matching respectively exist. For these complex systems, perfect positive (PP) means the free energies of the sites of the two components align in some way from high to low, while perfect negative (PN) means they misalign in some way with high free energy sites for one component aligning with low free energy sites for the other component. Other variations of PP and PN exist where the free energies correlate in some way with the free energy of the site of one of the components distributed among two or more sites of the other component, and uncorrelated exit where the free energies do not correlate but possibly still have some site distribution. A consistent set of single and binary isotherms for CO_2 and N_2 on 13X zeolite were used to explore all 19 correlations. CO_2 fitted well only to the TPL single gas model and N_2 fitted equally well to either the DPL or SPL single gas model. Only 3 of the 12 cases for the TPL–DPL model and 2 of the 7 cases for the TPL–SPL model exhibited reasonable predictions of the experimental results; the remaining 14 cases failed. The predictions for CO_2 for both models were very good for all 19 cases; but, some of the predictions for N_2 were so overpredicted, they were not even close to reality. The simpler site matching correlations fared better than the more complex ones, such as those with the sites of N_2 distributed over two or more sites of CO_2. For this CO_2–N_2-13X binary system, PP site matching correlations provided the best predictions, with the high and low free energy sites of N_2 decidedly interacting with the high and medium free energy sites of CO_2 with the low free energy site of CO_2 unoccupied by N_2.

List of symbols

A	Component A
b_i	Affinity parameter of component i ($=$ A or B), kPa^{-1}
β_i	Parameter defined in Eq. 13

✉ James A. Ritter
  ritter@cec.sc.edu

1 Department of Chemical Engineering, University of South Carolina, Columbia, SC 29208, USA

$b_{j,i}$	Affinity parameter of component i ($=$ A or B) on *Site j* ($=$ 1 or 2), kPa^{-1}
$b_{o,i,j}$	Pre-exponential factor of component i (A or B) on *Site j* ($=$ 1 or 2), kPa^{-1}
B	Component B
$E_{j,i}$	Adsorption energy of component i ($=$ A or B) on *Site j* ($=$ 1 or 2), kJ mol^{-1}
n_m	Total amount adsorbed from gas mixture, mol kg^{-1}
n_i	Amount adsorbed of component i ($=$ A or B) from single gas, mol kg^{-1}
$n_{i,m}$	Amount adsorbed of component i ($=$ A or B) from gas mixture, mol kg^{-1}
$n^s_{j,i}$	Saturation capacity of component i ($=$ A or B) on *Site j* ($=$ 1 or 2), mol kg^{-1}
n^s_i	Saturation capacity of component i ($=$ A or B), mol kg^{-1}

N Number of data points
P Absolute pressure, kPa
R Universal gas constant, kJ mol^{-1} K^{-1}
T Absolute temperature, K
x_i Adsorbed phase mole fraction of component i ($=$ A or B)
y_i Gas phase mole fraction of component i ($=$ A or B)
z_e Experimental quantity in Eq. 23
z_p Predicted quantity in Eq. 23

1 Introduction

Everyone who models cyclic adsorption processes for gas separation and purification requires a theorectical framework that reliably predicts mixed gas adsorption equilibria. Desirable features of such a model should include being simple to use, being explicit in the component amounts adsorbed and requiring only single component information for predicting mixed gas adsorption. The dual process Langmuir (DPL) model may be the only model that not only meets these requirements, but, as a bonus, it also has been shown to accurately predict mixed gas adsorption equilibria for a wide variety of systems including nonideal behavior like azeotropes [7]. This unique ability of the DPL model stems from its formulation being applicable to energetic site matching [7], with the concept of energetic site matching for other models first introduced independently by Valenzuela et al. [10] and Moon and Tien [5] as articulated by Cerofolini and Rudzinski [1].

Although the DPL model has been used for some time [6], it was shown only recently by Ritter et al. [7] how to carefully and correctly assign the free energies of each component on each site for predicting mixed gas adsorption equilibria. Since that time the DPL model and its varients have been gaining in popularity for predicting mixed gas adsorption equilibria in adsorption process simulation [8]. However, it is clear from this recent review that not everyone has considered energetic site matching when using the DPL model. The issue is that if the practice of energetic site matching with the DPL model is unintentionally ignored, erroneous predictions may be obtained because the adsorption free energies for each component on each site are not properly matched or alligned. These eroneous predictions have been shown for gas mixtures with the single gas isotherms of each component in the gas mixture all fitted well to the DPL model [7], or even with the single gas isotherms of one of the components in a binary gas mixture fitted well to the DPL model and the other compoonent fitted well to the single process Langmuir (SPL) model [8].

These DPL–DPL [7] and DPL–SPL [8] cases are very subtle because they result in different energetic site matching

situations that must be considered. The latter situation arises because in some cases just one type of site is required to fit the single gas isotherms like for O_2 on 5A zeolite [9]. But, what if the single gas isotherms are more nonlinear and thus require three types of sites to fit the data like for CO_2 on 13X zeolite [4]? Some even more interesting and equally subtle situations arise when the single gas isotherms of one of the components in a binary gas mixture are described by the three process Langmuir (TPL) model and the single gas isotherms of the other component are described by either the DPL or SPL model. These TPL–DPL and TPL–SPL systems have never been analyzed in the literature.

Therefore, the objective of this work is to formulate and evaluate all possible scenarios for predicting mixed gas adsorption equilibria of a binary gas mixture using the TPL–DPL and TPL–SPL models. These two scenarios differ from the previously studied DPL–DPL [7] and DPL–SPL [8] systems by how the free energies of each component on each site correlate with each other, i.e., by how the energetic site matching is carried out. In previous studies, perfect positive (PP), perfect negative (PN) and unselective (US) energetic site matching correlations were introduced. Because of the complexity of the TPL–DPL and TPL–SPL systems, additional correlations are introduced here based on the different energetic site matching permutations that exist. In additon to PP and PN, these include uncorrelated (UC), positive unselective (PUS), negative unselective (NUS) and uncorrelated unselective (UCUS). For both models, a consistent set of single and binary adsorption equilibira for CO_2 and N_2 on 13X zeolite [2] is used to elucidate these uniquely different scenarios. With extension now beyond the DPL model, these mixed gas adsorption equilibria formulations collectively deserve a more general name and are now called the multi-process Langmuir (MPL) model.

2 Multi-process Langmuir (MPL) model formulations

2.1 Unary equilibria

The single gas MPL model describes the adsorption of component i on a heterogeneous adsorbent that is comprised of M types of homogeneous but energetically different patches (or sites). Assuming that the adsorbate-adsorbent free energy on each type of patch is constant, the amount adsorbed n_i of component i is given by

$$n_i = \sum_{j=1}^{M} \left(\frac{n_{j,i}^s b_{j,i} P}{1 + b_{j,i} P} \right)_{Site j} \tag{1}$$

where $n_{j,i}^s$ and $b_{j,i}$ are respectively the saturation capacity and affinity parameter on *Site j*, and *P* is the absolute pressure. All of the assumptions of the Langmuir model apply on each type of patch, and the *M* types of patches or sites do not interact with each other [3]. The affinity parameter or free energy for each type of site is expressed as

$$b_{j,i} = b_{o_{j,i}} exp\left(\frac{E_{j,i}}{RT}\right) \tag{2}$$

where the subscript *j* represents the free energy level of *Site j*. $E_{j,i}$ is the adsorption energy of component *i* on *Site j*, $b_{o_{j,i}}$ is the pre-exponential factor or adsorption entropy of component *i* on *Site j*, and *T* is the absolute temperature. Of interest to this work is when $M = 1$, 2 or 3 in Eq. 1.

2.2 Binary equilibria

When one of the components in a binary gas mixture is described by either the SPL or DPL model and the other component is described by the TPL model, several interesting cases arise with respect to energetic site matching. There are twelve energetic site matching permutations to consider for the TPL–DPL model and seven for the TPL–SPL model. This means there are 19 different ways to arrange the free energy b_{ij} of each component *i* on each *Site j*. These energetic site matching cases are very subtle, just like the DPL–DPL case treated by Ritter et al. [7], and the DPL–SPL and DPL–LI (linear isotherm) cases recently treated by Ritter et al. [8].

2.3 TPL$_A$–DPL$_B$ system

For the TPL$_A$–DPL$_B$ binary mixed gas model, when component A is described by the TPL model there are three types of sites each component can adsorb on and when component B is described by the DPL model there are two types of sites each component can adsorb on. This gives rise to twelve permutations of energetic site matching: three perfect positive (PP), three perfect negative (PN), two positive unselective (PUS), two negative unselective (NUS) and two uncorrelated unselective (UCUS), as shown in Table 1. For component A, *Sites 1*, *2* and *3* are respectively designated as high, medium and low free enegy sites, and for component B, *Sites 1* and *2* are respectively designated as high and low free enegy sites. As noticed from Table 1, PP means the free energies of the various sites of the two components align in some way from high to low, while PN means they misalign in some way with high free energy sites of one component aligning with low free energy sites of the other component. PUS and NUS mean the free energies correlate in some way with one site of component B distributed among two sites

Table 1 TPL–DPL energetic site matching correlations

Correlation	Case	Component	Free energy site pairing		
Perfect positive (PP)	1	A	$b_{1,A}$	$b_{2,A}$	$b_{3,A}$
		B	$b_{1,B}$	$b_{2,B}$	
	2	A	$b_{1,A}$	$b_{2,A}$	$b_{3,A}$
		B	$b_{1,B}$		$b_{2,B}$
	3	A	$b_{1,A}$	$b_{2,A}$	$b_{3,A}$
		B		$b_{1,B}$	$b_{2,B}$
Perfect negative (PN)	4	A	$b_{1,A}$	$b_{2,A}$	$b_{3,A}$
		B	$b_{2,B}$	$b_{1,B}$	
	5	A	$b_{1,A}$	$b_{2,A}$	$b_{3,A}$
		B	$b_{2,B}$		$b_{1,B}$
	6	A	$b_{1,A}$	$b_{2,A}$	$b_{3,A}$
		B		$b_{2,B}$	$b_{1,B}$
Positive unselective (PUS)	7	A	$b_{1,A}$	$b_{2,A}$	$b_{3,A}$
		B	$b_{1,B}$	$b_{1,B}$	$b_{2,B}$
	8	A	$b_{1,A}$	$b_{2,A}$	$b_{3,A}$
		B	$b_{1,B}$	$b_{2,B}$	$b_{2,B}$
Negative unselective (NUS)	9	A	$b_{1,A}$	$b_{2,A}$	$b_{3,A}$
		B	$b_{2,B}$	$b_{1,B}$	$b_{1,B}$
	10	A	$b_{1,A}$	$b_{2,A}$	$b_{3,A}$
		B	$b_{2,B}$	$b_{2,B}$	$b_{1,B}$
Uncorrelated unselective (UCUS)	11	A	$b_{1,A}$	$b_{2,A}$	$b_{3,A}$
		B	$b_{1,B}$	$b_{2,B}$	$b_{1,B}$
	12	A	$b_{1,A}$	$b_{2,A}$	$b_{3,A}$
		B	$b_{2,B}$	$b_{1,B}$	$b_{2,B}$

of component A. UCUS means the energies do not correlate in any meaningful manner, but with one site of component B still being distributed among two sites of component A.

For Example, component B, which has an affinity for two types of sites, can interact with the high and medium free energy sites of component A, the high and low free energy sites of component A, or the medium and low free energy sites of component A, all three cases (Cases 1, 2 and 3) in a PP fashion. Or, the low and high free energy sites of component B can intereact respectively with the high and medium free energy sites of component A, the high and low free energy sites of component A, or the medium and low free energy sites of component A, all three cases (Cases 4, 5 and 6) in a PN fashion. Or, the high free energy site of component B can intereact with both the high and medium free energy sites of component A while the low free energy site of component B can intereact with the low free energy site of component A, as in Case 7 in a PUS fashion. It should be obvious at this point as to how the NUS and UCUS cases are constructed. When component B interacts with only two sites of component A, then component B does not adsorb at all on one of the sites of component A. However, when component B interacts with all three sites of component A like in Cases

7 to 12, then it is assumed that the ratio of the saturation capacities of component B on the two distributed sites of component A is the same as that of component A on these sites, as shown below. A few quantitative examples follow.

For the TPL_A-DPL_B binary mixed gas model, when components A and B obey a PP correlation for energetic site matching according to Case 1 (Table 1), the corresponding amount adsorbed for each component from a binary gas mixture is given by

$$n_{A,m} = \left(\frac{n_{1,A}^s P y_A b_{1,A}}{1 + P y_A b_{1,A} + P y_B b_{1,B}} \right)_{Site1}$$
$$+ \left(\frac{n_{2,A}^s P y_A b_{2,A}}{1 + P y_A b_{2,A} + P y_B b_{2,B}} \right)_{Site2} + \left(\frac{n_{3,A}^s P y_A b_{3,A}}{1 + P y_A b_{3,A}} \right)_{Site3} \quad (3)$$

$$n_{B,m} = \left(\frac{n_{1,B}^s P y_B b_{1,B}}{1 + P y_A b_{1,A} + P y_B b_{1,B}} \right)_{Site1} + \left(\frac{n_{2,B}^s P y_B b_{2,B}}{1 + P y_A b_{2,A} + P y_B b_{2,B}} \right)_{Site2} \quad (4)$$

When components A and B obey a PN correlation for energetic site matching according to Case 4 (Table 1), the corresponding amount adsorbed for each component from a binary gas mixture is given by

$$n_{A,m} = \left(\frac{n_{1,A}^s P y_A b_{1,A}}{1 + P y_A b_{1,A} + P y_B b_{2,B}} \right)_{Site1}$$
$$+ \left(\frac{n_{2,A}^s P y_A b_{2,A}}{1 + P y_A b_{2,A} + P y_B b_{1,B}} \right)_{Site2} + \left(\frac{n_{3,A}^s P y_A b_{3,A}}{1 + P y_A b_{3,A}} \right)_{Site3} \quad (5)$$

$$n_{B,m} = \left(\frac{n_{1,B}^s P y_B b_{1,B}}{1 + P y_A b_{2,A} + P y_B b_{1,B}} \right)_{Site1} + \left(\frac{n_{2,B}^s P y_B b_{2,B}}{1 + P y_A b_{1,A} + P y_B b_{2,B}} \right)_{Site2} \quad (6)$$

where y_A and y_B are the gas phase mole fractions of components A and B, and $n_{A,m}$ and $n_{B,m}$ are the amounts adsorbed of components A and B from the binary gas mixture. When components A and B obey a PUS correlation for energetic site matching according to Case 8 (Table 1), the corresponding amount adsorbed for each component from a binary gas mixture is given by

$$n_{A,m} = \left(\frac{n_{1,A}^s P y_A b_{1,A}}{1 + P y_A b_{1,A} + P y_B b_{1,B}} \right)_{Site1}$$
$$+ \left(\frac{n_{2,A}^s P y_A b_{2,A}}{1 + P y_A b_{2,A} + P y_B b_{2,B}} \right)_{Site2} + \left(\frac{n_{3,A}^s P y_A b_{3,A}}{1 + P y_A b_{3,A} + P y_B b_{2,B}} \right)_{Site3} \quad (7)$$

$$n_{B,m} = \left(\frac{n_{1,B}^s P y_B b_{1,B}}{1 + P y_A b_{1,A} + P y_B b_{1,B}} \right)_{Site1}$$
$$+ \left(\frac{\beta_2 n_{2,B}^s P y_B b_{2,B}}{1 + P y_A b_{2,A} + P y_B b_{2,B}} \right)_{Site2} + \left(\frac{\beta_3 n_{2,B}^s P y_B b_{2,B}}{1 + P y_A b_{3,A} + P y_B b_{2,B}} \right)_{Site3} \quad (8)$$

where

$$\beta_2 + \beta_3 = 1 \quad (9)$$

and

$$\frac{\beta_2}{n_{2,A}^s} = \frac{\beta_3}{n_{3,A}^s} \quad (10)$$

Solving Eqs. 9 and 10 for β_2 and β_3 provides the distribution of $n_{2,B}^s$ for *Sites 2* and *3*. The total amount adsorbed n_m is simply the sum of $n_{A,m}$ and $n_{B,m}$. The adsorbed phase mole fractions of components A and B, i.e., x_A and x_B, are given by

$$x_A = \frac{n_{A,m}}{n_{A,m} + n_{B,m}} \quad (11)$$

$$x_B = \frac{n_{B,m}}{n_{A,m} + n_{B,m}} \quad (12)$$

In these formulations, the saturation capacity for each component on each type of site is allowed to be different with minimal consequences, as shown elsewhere [7].

2.4 TPL_A–SPL_B system

For the TPL_A–SPL_B binary mixed gas model, when component A is described by the TPL model there are three types of sites each component can adsorb on and when component B is described by the SPL model there is only one type of site each component can adsorb on. This gives rise to seven permutations of energetic site matching: one PP, one uncorrelated (UC), one PN, one PUS, one NUS and two UCUS, as shown in Table 2. For component A, *Sites 1*, *2* and *3* are respectively its high, medium and low free enegy sites, and for component B, *Site 1* is its only free enegy site.

Component B, which has an affinity for only one type of site, can interact solely with the high free energy site of component A in a PP fashion (Case 13), solely with the medium free energy site of component A in an UC fashion (Case 14), with UC simply meaning the energies of the various sites of the two components do not correlate. Or, component B can interact solely with the low free energy site of component A in a PN fashion (Case 15). Or, component B can intereact with just two types of sites of component A again with the same affinity on each type of site, i.e., component B can intereact with the high and medium free energy sites of component A in a PUS fashion (Case 16), medium and low free energy sites of component A in a NUS fashion (Case 17), or high and low free energy sites of component A in a UCUS fashion (Case 18). Or, component B can intereact with all three types of sites of component A with the same affinity on each type of site in an UCUS fashion (Case 19). Clearly, when component B interacts with only one or two sites of

Table 2 TPL–SPL energetic site matching correlations

Correlation	Case	Component	Free energy site pairing		
Perfect positive (PP)	13	A	$b_{1,A}$	$b_{2,A}$	$b_{3,A}$
		B	$b_{1,B}$		
Uncorrelated (UC)	14	A	$b_{1,A}$	$b_{2,A}$	$b_{3,A}$
		B		$b_{1,B}$	
Perfect negative (PN)	15	A	$b_{1,A}$	$b_{2,A}$	$b_{3,A}$
		B			$b_{1,B}$
Positive unselective (PUS)	16	A	$b_{1,A}$	$b_{2,A}$	$b_{3,A}$
		B	$b_{1,B}$	$b_{1,B}$	
Negative unselective (NUS)	17	A	$b_{1,A}$	$b_{2,A}$	$b_{3,A}$
		B		$b_{1,B}$	$b_{1,B}$
Uncorrelated unselective (UCUS)	18	A	$b_{1,A}$	$b_{2,A}$	$b_{3,A}$
		B	$b_{1,B}$		$b_{1,B}$
	19	A	$b_{1,A}$	$b_{2,A}$	$b_{3,A}$
		B	$b_{1,B}$	$b_{1,B}$	$b_{1,B}$

component A, then component B does not adsorb at all on the other sites of component A. When component B interacts with two or three sites of component A, then it is assumed that the ratio of the saturation capacities of component B on the distributed sites of component A is the same as that of component A on these sites, as shown below. A few quantitative examples follow.

For the TPL_A–SPL_B binary mixed gas model, when components A and B obey a PP correlation for energetic site matching according to Case 13 (Table 2), the corresponding amount adsorbed for each component from a binary gas mixture is given by

$$n_{A,m} = \left(\frac{n_{1,A}^s P y_A b_{1,A}}{1 + P y_A b_{1,A} + P y_B b_B} \right)_{Site1}$$
$$+ \left(\frac{n_{2,A}^s P y_A b_{2,A}}{1 + P y_A b_{2,A}} \right)_{Site2} + \left(\frac{n_{3,A}^s P y_A b_{3,A}}{1 + P y_A b_{3,A}} \right)_{Site3} \quad (13)$$

$$n_{B,m} = \left(\frac{n_B^s P y_B b_B}{1 + P y_A b_{1,A} + P y_B b_B} \right)_{Site1} \quad (14)$$

When components A and B obey an UC correlation for energetic site matching according to Case 14 (Table 2), the corresponding amount adsorbed for each component from a binary gas mixture is given by

$$n_{A,m} = \left(\frac{n_{1,A}^s P y_A b_{1,A}}{1 + P y_A b_{1,A}} \right)_{Site1}$$
$$+ \left(\frac{n_{2,A}^s P y_A b_{2,A}}{1 + P y_A b_{2,A} + P y_B b_B} \right)_{Site2} + \left(\frac{n_{3,A}^s P y_A b_{3,A}}{1 + P y_A b_{3,A}} \right)_{Site3} \quad (15)$$

$$n_{B,m} = \left(\frac{n_B^s P y_B b_B}{1 + P y_A b_{2,A} + P y_B b_B} \right)_{Site2} \quad (16)$$

When components A and B obey a PN correlation for energetic site matching according to Case 15 (Table 2), the corresponding amount adsorbed for each component from a binary gas mixture is given by

$$n_{A,m} = \left(\frac{n_{1,A}^s P y_A b_{1,A}}{1 + P y_A b_{1,A}} \right)_{Site1}$$
$$+ \left(\frac{n_{2,A}^s P y_A b_{2,A}}{1 + P y_A b_{2,A}} \right)_{Site2} + \left(\frac{n_{3,A}^s P y_A b_{3,A}}{1 + P y_A b_{3,A} + P y_B b_B} \right)_{Site3} \quad (17)$$

$$n_{B,m} = \left(\frac{n_B^s P y_B b_B}{1 + P y_A b_{3,A} + P y_B b_B} \right)_{Site3} \quad (18)$$

When components A and B obey a UCUS correlation for energetic site matching according to Case 19 (Table 2), the corresponding amount adsorbed for each component from a binary gas mixture is given by

$$n_{A,m} = \left(\frac{n_{1,A}^s P y_A b_{1,A}}{1 + P y_A b_{1,A} + P y_B b_B} \right)_{Site1}$$
$$+ \left(\frac{n_{2,A}^s P y_A b_{2,A}}{1 + P y_A b_{2,A} + P y_B b_B} \right)_{Site2} + \left(\frac{n_{3,A}^s P y_A b_{3,A}}{1 + P y_A b_{3,A} + P y_B b_B} \right)_{Site3} \quad (19)$$

$$n_{B,m} = \left(\frac{\beta_1 n_B^s P y_B b_B}{1 + P y_A b_{1,A} + P y_B b_B} \right)_{Site1}$$
$$+ \left(\frac{\beta_2 n_B^s P y_B b_B}{1 + P y_A b_{2,A} + P y_B b_B} \right)_{Site2} + \left(\frac{\beta_3 n_B^s P y_B b_B}{1 + P y_A b_{3,A} + P y_B b_B} \right)_{Site3} \quad (20)$$

where

$$\beta_1 + \beta_2 + \beta_3 = 1 \quad (21)$$

and

$$\frac{\beta_1}{n_{1,A}^s} = \frac{\beta_2}{n_{2,A}^s} = \frac{\beta_3}{n_{3,A}^s} \quad (22)$$

Solving Eqs. 21 and 22 for β_1, β_2 and β_3 provides the distribution of n_B^s for *Sites 1*, *2* and *3*. Again, in these formualtions the total amount adsorbed is simply the sum of $n_{A,m}$ and $n_{B,m}$, the adsorbed phase mole fractions of components A and B, i.e., x_A and x_B, are given by Eqs. 11

and 12, and the saturation capacity for each component on each type of site is allowed to be different.

3 Results and discussion

3.1 Single component correlations

To illustrate the utility and diversity of the TPL–DPL and TPL–SPL formulations, a consistent set of single and binary adsorption isotherms from the literature were selected, i.e., CO_2 and N_2 on 13X zeolite [2]. To determine if one, two or three processes were needed for each component, the single component equilibrium adsorption isotherms for CO_2 and N_2 on 13X zeolite were fitted in order to the single component SPL, DPL and TPL models using Eq. 1 reduced to the corresponding number of sites, along with Eq. 2. For each adsorbate, the isotherms measured at all five temperatures

were fitted simultaneously to each model using Excel Solver with the fitting parameters scaled so their magnitudes ranged between 0.1 and 10 for Solver to work most effectively. The resulting model parameters are summarized in Table 3 and Figs. 1 and 2. Also included in this table are the affinity parameters for the various sites, i.e., the $b_{j,i}$ in Eq. 1 for each site of each component for two temperatures based on the mixed gas data. They were computed from the parameters in Table 3 using Eq. 2. These $b_{j,i}$ are ordered from largest to smallest and respectively assigned to *Site 1*, *Sites 1 and 2*, or *Sites 1, 2 and 3* for the SPL, DPL and TPL models, respectively.

The goodness of the fit of each model was judged by the average relative error (ARE) defined as

$$ARE = \frac{100}{N} \sum_i^N abs\left(\frac{z_e - z_p}{z_e}\right)_i \tag{23}$$

Table 3 Single-process Langmuir (SPL), dual-process Langmuir (DPL) and three process Langmuir (TPL) model parameters, average relative errors (AREs) and R^2 values (coefficients of determination) obtained from fitting single component adsorption isotherms of CO_2 and N_2 on 13X zeolite [2]

Model	SPL		DPL		TPL	
Adsorbate/parameter	CO_2	N_2	CO_2	N_2	CO_2	N_2
b_{o_1} (kPa^{-1})	–	6.313×10^{-7}	1.870×10^{-7}	2.877×10^{-6}	5.327×10^{-8}	–
E_1 (kJ mol^{-1})	–	18.548	39.098	16.122	45.398	–
b_1 25 °C (kPa^{-1})	–	1.121×10^{-3}	$1.324 \times 10^{+0}$	1.921×10^{-03}	$4.790 \times 10^{+0}$	–
b_1 45 °C (kPa^{-1})	–	7.007×10^{-4}	4.914×10^{-1}	1.276×10^{-03}	$1.515 \times 10^{+0}$	–
n_1^s (mol kg^{-1})	–	3.774	3.411	0.811	2.122	–
b_{o_2} (kPa^{-1})	–	–	3.533×10^{-8}	3.003×10^{-7}	9.209×10^{-8}	–
E_2 (kJ mol^{-1})	–	–	33.509	19.737	35.030	–
b_2 25 °C (kPa^{-1})	–	–	2.624×10^{-2}	8.620×10^{-04}	1.263×10^{-1}	–
b_2 45 °C (kPa^{-1})	–	–	1.122×10^{-2}	5.226×10^{-04}	5.197×10^{-2}	–
n_2^s (mol kg^{-1})	–	–	2.826	3.181	3.022	–
b_{o_3} (kPa^{-1})	–	–	–	–	4.495×10^{-9}	–
E_3 (kJ mol^{-1})	–	–	–	–	33.776	–
b_3 25 °C (kPa^{-1})	–	–	–	–	3.757×10^{-3}	–
b_3 45 °C (kPa^{-1})	–	–	–	–	1.594×10^{-3}	–
n_3^s (mol kg^{-1})	–	–	–	–	1.578	–
ARE (%)	–	2.13	2.55	0.99	0.74	–
R^2	–	0.99991	0.99761	0.99998	0.99973	–

where N is the total number of data points for each adsorbate, and z_e and z_p are respectively the experimental and predicted quantities of interest, in this case the amount adsorbed $n_{i,m}$. It was also judged by the coefficient of determination (R^2 values). It was clear from the AREs and R^2 values that the CO_2 isotherms fitted well only to the TPL model (SPL results not shown), while the N_2 isotherms fitted equally well to either the SPL or DPL model (TPL results not shown), especially based on the R^2 values, where a fitting that achieves at least four nines is considered the same. This raises an interesting dilemma for N_2 in choosing either the SPL or DPL model for mixed gas adsorption prediction with CO_2. This quandary spawned the analysis and comparison contained in this work, i.e., exploring the predictions from the TPL_{CO2}–DPL_{N2} and TPL_{CO2}–SPL_{N2} binary mixed gas models.

Predictions from the single component Langmuir models, plotted along with the experimental isotherms in Figs. 1 and 2 respectively for CO_2 and N_2, reflect very well the AREs
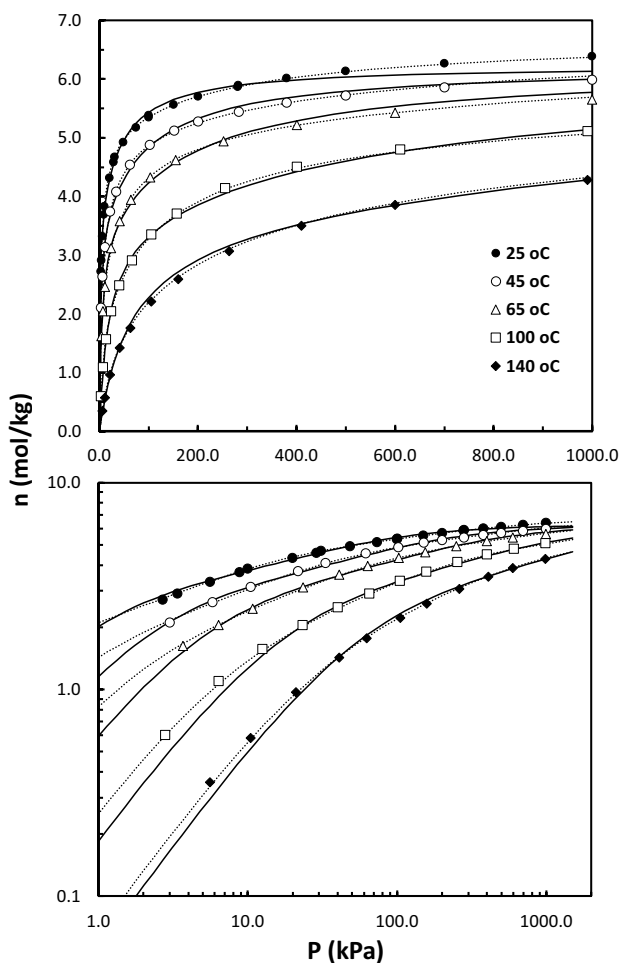
Fig. 1 Single gas equilibrium adsorption isotherms for CO_2 on 13X zeolite [2] fitted to the DPL (solid lines) and TPL (dotted lines) models, showing the correlations in both linear–linear and log–log scales; model parameters and goodness of fits are provided in Table 3
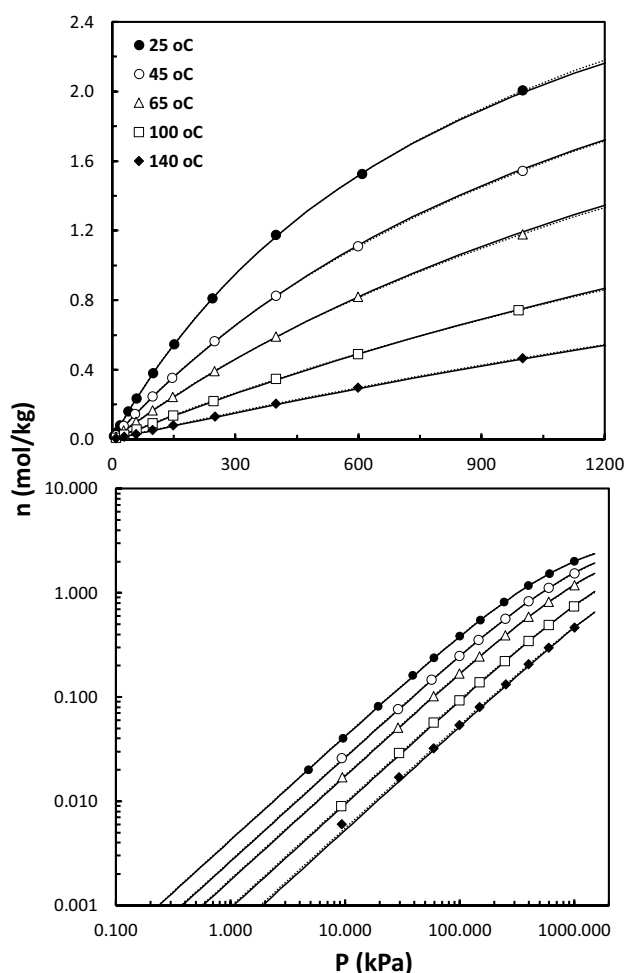
Fig. 2 Single gas equilibrium adsorption isotherms for N_2 on 13X zeolite [2] fitted to the SPL (solid lines) and DPL (dotted lines) models, showing the correlations in both linear–linear and log–log scales; model parameters and goodness of fits are provided in Table 3

and R^2 values in Table 3. Nearly perfect and indistinguishable agreement was obtained for each isotherm of N_2 using the SPL and DPL models. Notice the ARE and R^2 values from the DPL model are only slightly better than those from the SPL model for N_2. This indicated someone doing a regression analysis without much consideration or insight might use either formulation for N_2, resulting in significantly different predictions of mixed gas adsorption with CO_2 in some cases, as shown below. However, only the TPL model was capable of fitting the CO_2 isotherms, with nearly perfect agreement. In contrast, the DPL model revealed obvious discrepancies between the experimental data and the model, making the TPL model for CO_2 any easy choice for mixed gas predictions with N_2.

3.2 Binary adsorption equilbria predictions

For the TPL–DPL and TPL–SPL binary models, all 21 experimental binary adsorption equilibrium data points for the CO_2–N_2-13X system [2] were used to compare the predictions from each of the 19 different site matching correlations (cases) in Tables 1 and 2. This binary data set was obtained at two temperatures ($T = 25$ and 45 °C) and three pressures ($P = 1.2$, 3.1 and 10.1 bar) over a range of gas phase CO_2 mole fractions ($y_{CO_2} = 0.002$ to 0.701). The results are summarized in Tables 4 and 5 respectively in terms of the average relative errors (AREs) of the component loading and component mole fraction predictions from the TPL–DPL and TPL–SPL for each of the 19 cases for all data points at each temperature. The italic values in Tables 4 and 5 were considered the cases with the best predictions, while the bold values were considered the cases with the worst predictions for both the TPL–DPL and TPL–SPL models. *n-y* and *x–y* diagrams for these select 7 cases are shown in Figs. 3, 4, 5, 6, 7, 8 and 9 for the TPL–DPL model and in Figs. 10, 11, 12 and 13 for the TPL–SPL model. The average AREs for each pressure and temperature for each case are tabulated and provided in Supplemental Information in Tables S1 and S2 respectively for the component loadings and component mole fractions. The *n-y* and *x–y* diagrams for

Table 4 Average of the average relative errors (AREs) of the component loading predictions from the TPL–DPL and TPL–SPL for all site matching correlations (cases) for all pressures and at each temperature of the binary adsorption equilibria of CO_2 and N_2 on 13X zeolite [2]: italic values considered best predictions, bold values considered worst predictions

Model	Case	CO₂ 25 °C	N₂ 25 °C	CO₂ 45 °C	N₂ 45 °C
TPL–DPL	*1*	*4.1*	*33.8*	*3.8*	*39.4*
	2	3.7	525.5	3.7	390.3
	3	**1.8**	**567.5**	**1.8**	**443.5**
	4	*3.1*	*45.8*	*2.3*	*46.6*
	5	3.2	221.5	3.7	175.5
	6	1.9	298.5	2.4	259.9
	7	3.0	550.1	2.7	421.5
	8	3.1	254.4	3.2	195.3
	9	*2.7*	*62.2*	*2.3*	*63.5*
	10	2.4	266.1	2.5	222.6
	11	3.0	127.4	2.7	115.1
	12	2.4	195.5	2.2	150.0
TPL–SPL	13	4.6	85.7	4.9	83.6
	14	*2.9*	*51.4*	*3.1*	*69.0*
	15	**2.9**	**826.1**	**4.0**	**640.3**
	16	*3.6*	*40.5*	*3.2*	*45.6*
	17	1.9	177.4	2.3	148.5
	18	3.4	303.1	4.2	226.8
	19	2.6	181.9	2.5	150.1

Table 5 Average of the average relative errors (AREs) of the component mole fraction predictions from the TPL–DPL and TPL–SPL for all site matching correlations (cases) for all pressures and at each temperature of the binary adsorption equilibria of CO_2 and N_2 on 13X zeolite [2]: italic values considered best predictions, bold values considered worst predictions

Model	Case	CO₂ 25 °C	N₂ 25 °C	CO₂ 45 °C	N₂ 45 °C
TPL–DPL	*1*	*2.3*	*33.8*	*0.9*	*39.5*
	2	6.3	482.7	4.8	350.3
	3	**7.7**	**524.3**	**6.5**	**404.3**
	4	*1.5*	*46.3*	*1.2*	*45.4*
	5	1.9	213.9	1.8	164.8
	6	4.7	283.0	4.0	241.1
	7	5.5	511.6	6.1	387.4
	8	3.3	241.5	2.7	182.0
	9	*1.3*	*62.7*	*0.8*	*62.2*
	10	3.4	255.4	3.0	209.0
	11	3.2	123.4	2.1	109.7
	12	1.9	189.3	1.9	142.7
TPL–SPL	13	2.5	84.6	3.0	82.7
	14	*3.0*	*45.8*	*1.9*	*62.5*
	15	**9.5**	**738.9**	**7.9**	**557.3**
	16	*1.2*	*42.2*	*1.2*	*44.7*
	17	2.2	170.0	2.0	138.6
	18	2.5	285.6	2.2	207.2
	19	2.9	174.5	2.2	141.4

the remaining 12 cases are also provided in Supplemental Information in Figures S1 to S12. The predictions from the TPL–DPL are discussed first, followed by those from the TPL–SPL model.

3.3 TPL–DPL model predictions

There were 12 energetic site matching correlations to consider for the TPL–DPL model: three perfect positive (PP), three perfect negative (PN), two positive unselective (PU), two negative unselective (NU) and two uncorrelated unselective (UCUS). For the PP and PN cases, the two N_2 sites occupied only two of the three CO_2 sites, leaving one of the CO_2 sites unoccupied by N_2. In contrast, for the PUS, NUS and UCUS cases, the two N_2 sites occupied all three CO_2 sites in one fashion or another, with one of the N_2 sites being split between two of the CO_2 sites according to a form of Eqs. 9 and 10, depending on the correlation. For this CO_2–N_2-13X binary system, intuition suggested for energetic site matching that PP implies the higher free enegy sites of CO_2 would align with the higher free enegy sites of N_2, because they both have quadrupole moments that interact with the Na ions in the 13X [11]. Conversely, PN implies that the higher free enegy sites of CO_2 would align with the lower free energy sites of N_2. With these
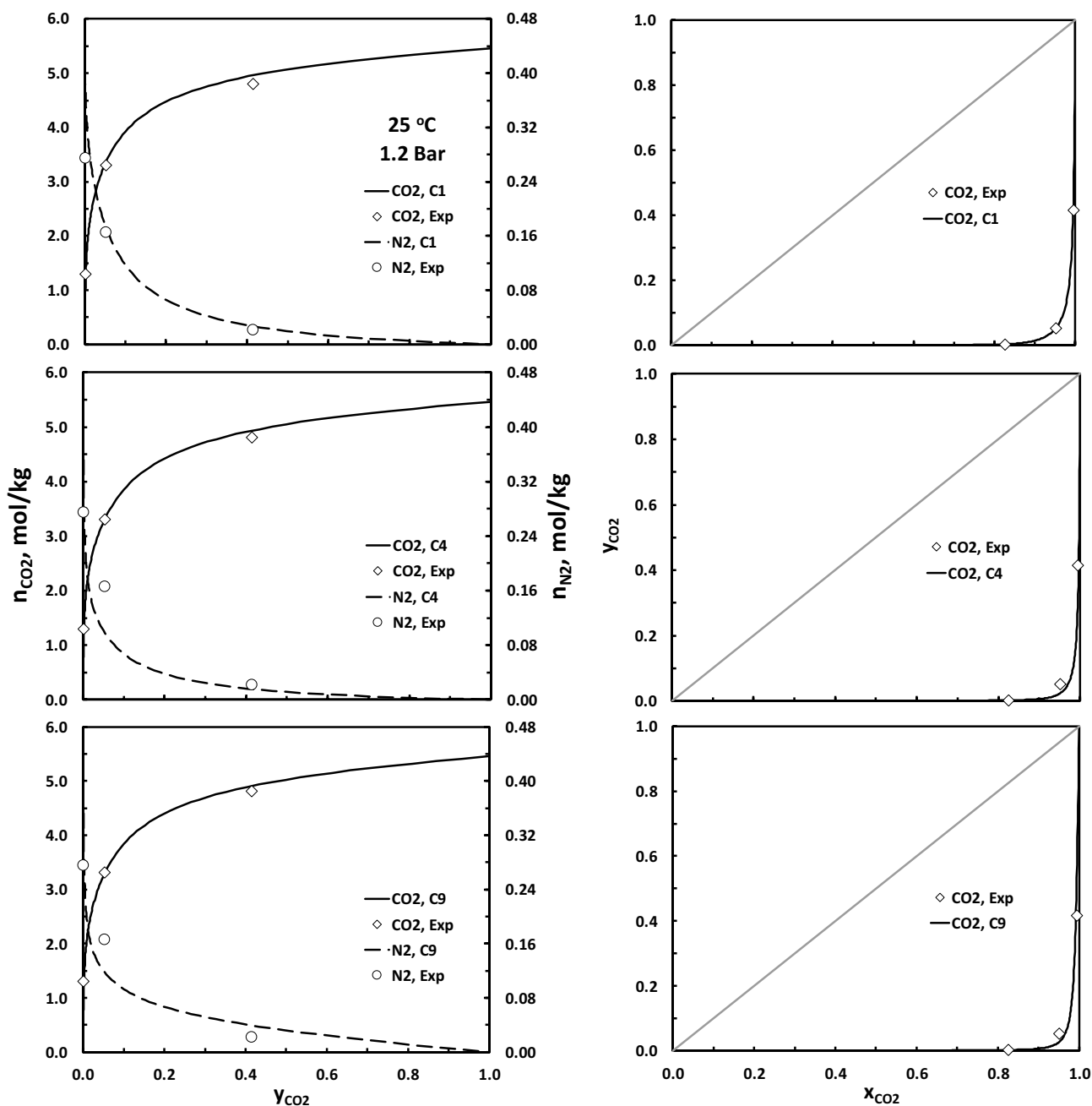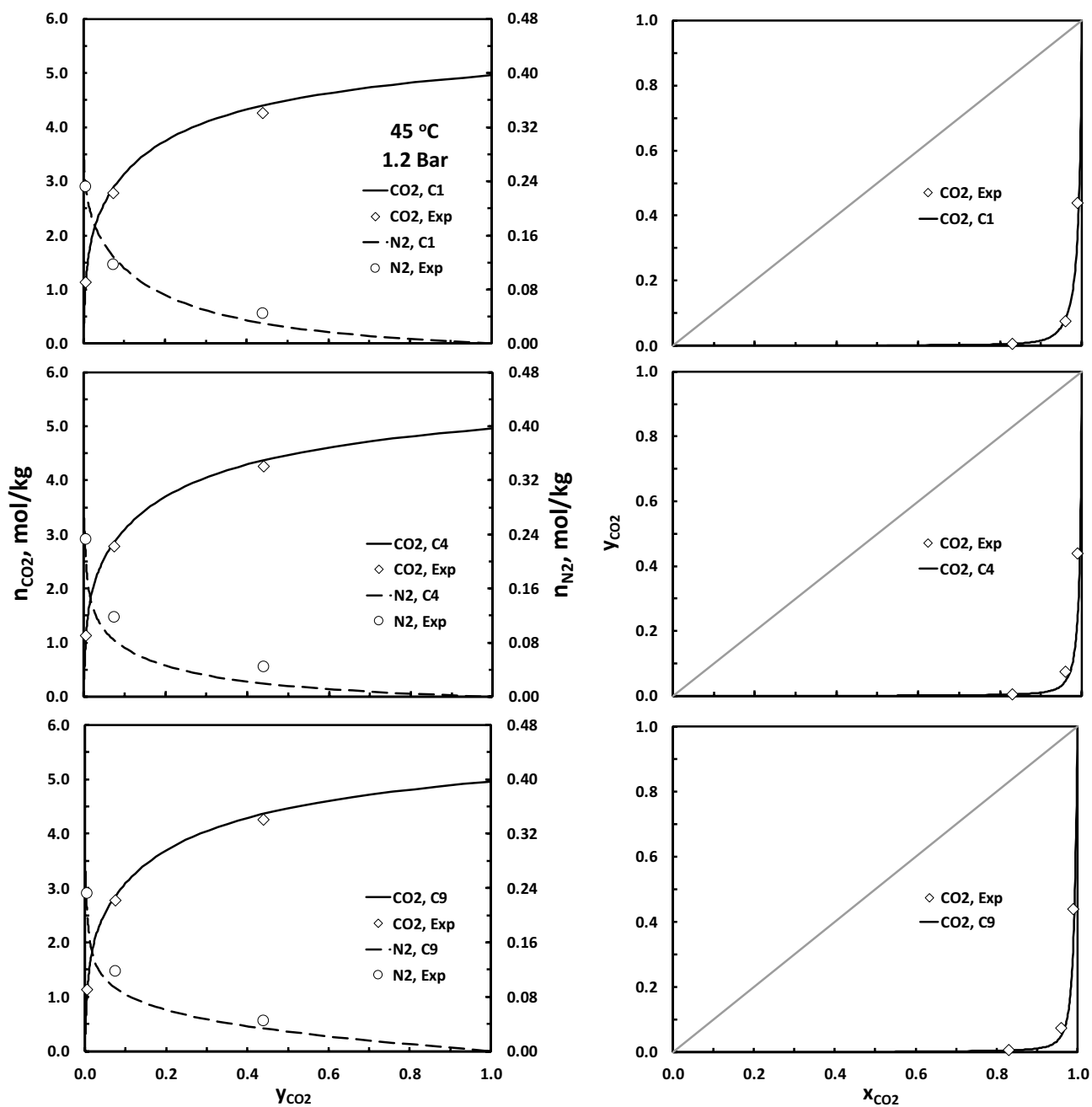
Fig. 3 Comparison of binary predictions (lines) of n–y and x–y mixed gas adsorption equilibria (symbols, Exp) for CO_2 and N_2 on 13X zeolite at $T = 25$ °C and $P = 1.2$ bar by the TPL_{CO_2}–DPL_{N_2} model for Cases 1 (perfect positive, C1), 4 (perfect negative, C4) and 9 (negative unselective, C9) in Table 1

definitions in mind, one of the positive site matching correlations, i.e., Cases 1, 2, 3, 7 or 8, was expected to provide the best predictions for this CO_2–N_2-13X binary system. The results were quite interesting and somewhat unexpected.

Only three of the 12 cases for the TPL–DPL model exhibited similar and reasonable predictions of the experimental results for both the component loadings (Table 4) and

component mole fractions (Table 5). These were Cases 1, 4 and 9. Although the AREs for CO_2 were relatively small for all 12 cases (all being less than 5% for the CO_2 loadings and less than 8% for the CO_2 mole fractions), those for N_2 were markedly different (ranging between 34 and 568% for the N_2 loadings, and between 34 and 524% for the N_2 mole fractions). Thus, the other 9 cases completely failed in predicting both the N_2 loadings and N_2 mole fractions, with

Fig. 4 Comparison of binary predictions (lines) of n–y and x–y mixed gas adsorption equilibria (symbols, Exp) for CO_2 and N_2 on 13X zeolite at $T = 45\ °C$ and $P = 1.2$ bar by the TPL_{CO2}–DPL_{N2} model for Cases 1 (perfect positive, C1), 4 (perfect negative, C4) and 9 (negative unselective, C9) in Table 1

Case 3 perhaps considered as the worst correlation, based on the N_2 predictions. The disparity beteen the CO_2 and N_2 predictions even for Cases 1, 4 and 9 was not surprising. Since the CO_2 to N_2 selectivity is very high, thereby causing the N_2 loadings and mole fractions to be relatively small, it was expected that N_2 would realize large errors just based on the definiton of the ARE (Eq. 23).

Figure 3 compares binary predictions from the TPL–DPL model at $T = 25\ °C$ and $P = 1.2$ bar in terms of n–y and x–y diagrams for Cases 1, 4 and 9, the three best cases. Figures 4, 5, 6, 7, and 8 show the same information, but each at a different temperature and pressure, covering all the binary data for the CO_2–N_2-13X system [2]. To exemplify how bad the predictions might become from the TPL–DPL model, because the adsorption free energies for each component
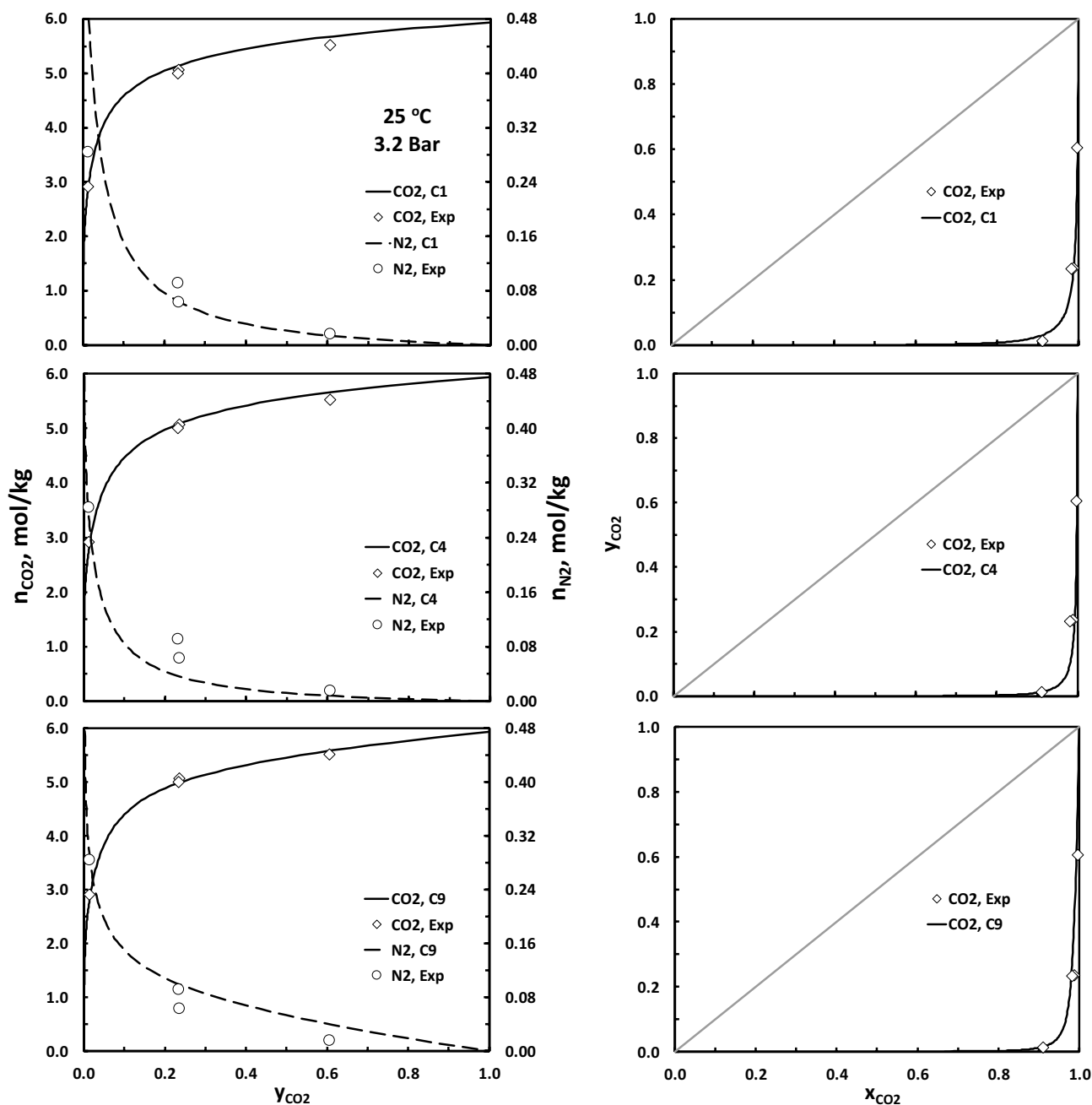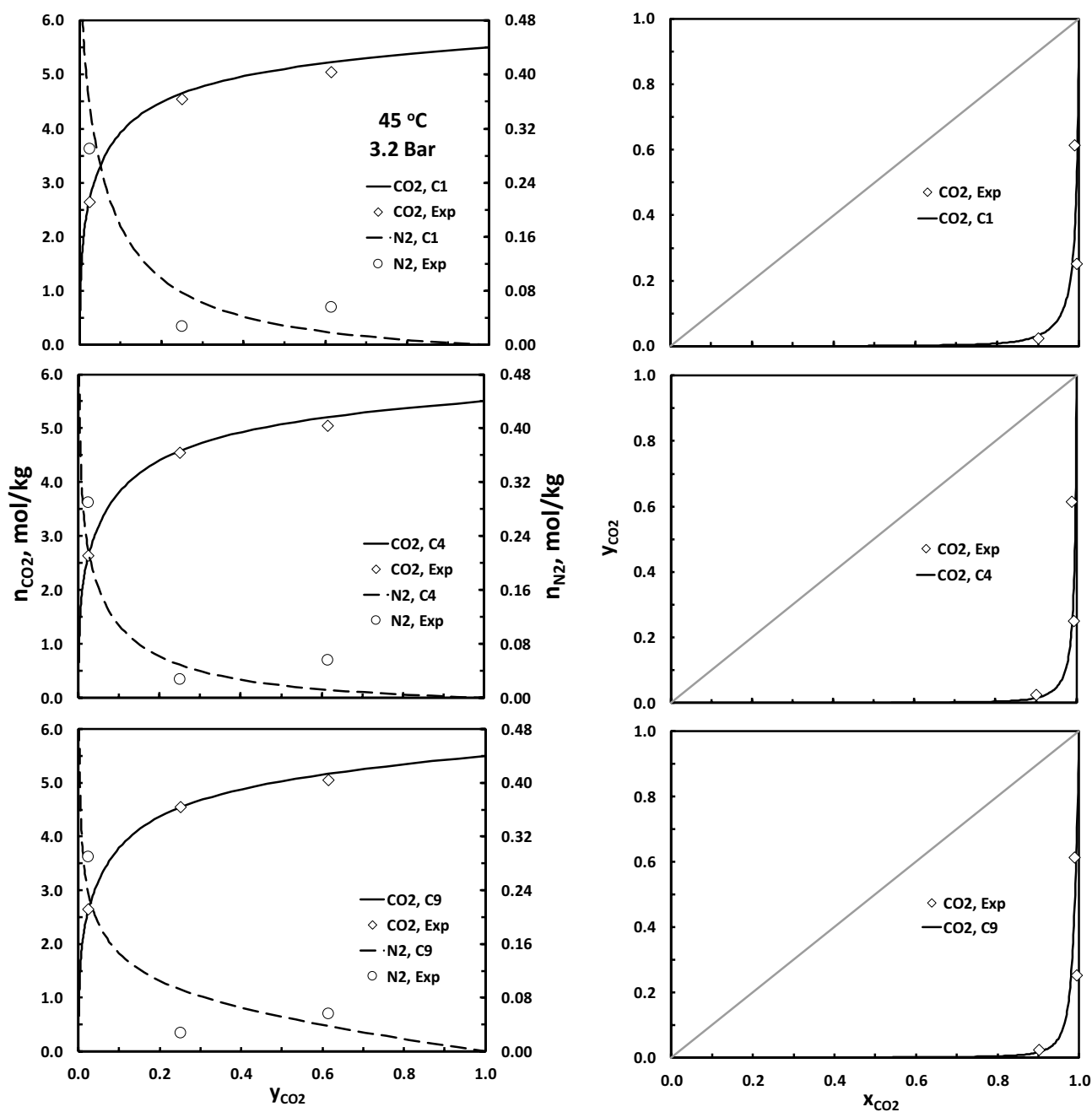
Fig. 5 Comparison of binary predictions (lines) of n–y and x–y mixed gas adsorption equilibria (symbols, Exp) for CO_2 and N_2 on 13X zeolite at $T = 25$ °C and $P = 3.2$ bar by the TPL_{CO_2}–DPL_{N_2} model for Cases 1 (perfect positive, C1), 4 (perfect negative, C4) and 9 (negative unselective, C9) in Table 1

on each site are not correct, Fig. 9 shows the n–y and x–y diagrams for Case 3, perhaps the worst case of all 12 cases based on the AREs in Tables 4 and 5 for the TPL–DPL model.

In all three cases in Figs. 3, 4, 5, 6, 7 and 8 the predictions of the x–y diagrams compared well with the experimental data, except for those in Fig. 7 at $T = 25$ °C and $P = 10.1$ bar. For some reason, the model underpredicted

one of the experimental data points for N_2 to about the same extent in each case, tending to suggest there might be an issue with this data point or that the model, even with the unselective conditions provided in Eqs. 9 and 10, is too restrictive to accurately predict the adsorption of N_2 at elevated pressures. Lateral interactions between the molecules in the zeolite cages might also be playing a role at these conditions, which are not accounted for in these
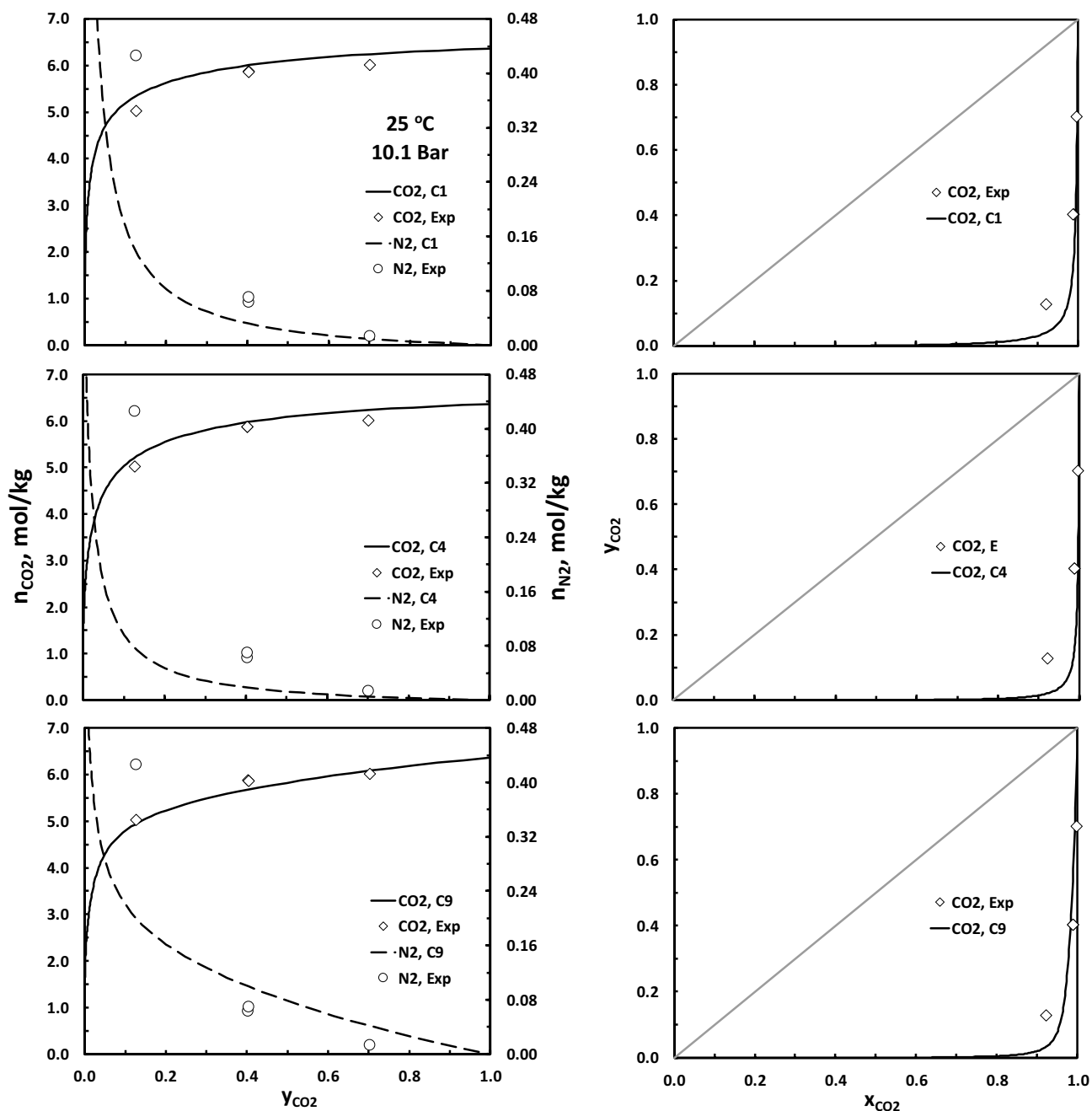
Fig. 6 Comparison of binary predictions (lines) of n–y and x–y mixed gas adsorption equilibria (symbols, Exp) for CO_2 and N_2 on 13X zeolite at $T = 45\ °C$ and $P = 3.2$ bar by the TPL_{CO2}–DPL_{N2} model for Cases 1 (perfect positive, C1), 4 (perfect negative, C4) and 9 (negative unselective, C9) in Table 1

Langmuir formulations. Also, in all three cases the predictions of the n–y diagram for CO_2 were very good, which is reflected in the relatively small AREs in Table 4. This was not the situation for the n–y diagram for N_2, where the deviations between experiment and model were much more pronounced, especially for Cases 4 and 9. Case 1, the best case according to the AREs in Tables 4 and 5, exhibited only small deviations between experiment and model

for N_2, while the model predictions for Cases 4 and 9 deviated significantly and similarly from experiment. The fact that the marked deviations exhibited by Cases 4 and 9 were similar to each other was perhaps due to their energetic site matching correlations being similar (Table 1).

Figure 9 compares experiment with TPL–DPL model preditions at two different pressures and temperatures for the worst Case 3. In this case, the x–y diagrams were

Fig. 7 Comparison of binary predictions (lines) of n–y and x–y mixed gas adsorption equilibria (symbols, Exp) for CO_2 and N_2 on 13X zeolite at $T = 25$ °C and $P = 10.1$ bar by the TPL_{CO2}–DPL_{N2} model for Cases 1 (perfect positive, C1), 4 (perfect negative, C4) and 9 (negative unselective, C9) in Table 1

strikingly overpredicted by the model, as were the n–y diagrams for N_2 to the point where the model was not even close to reality. These erroneous results could happen if the wrong correlation is inadvertently chosen or if the practice of energetic site matching is unintentionally ignored and the sites are assigned randomly. Not surprisingly, the model predictions of the n–y diagrams for CO_2 for this Case 3 were very good, just like for the best Cases

1, 4 and 9. This was true for all 12 cases, irrespective of the site matching corrleation, because N_2 simply does not affect the adsorption of CO_2 on 13X; but, the N_2 predictions might be very bad because CO_2 does affect the adsorption of N_2 on 13X.

Case 1 resulted in the smallest ARE overall, in agreement with the supposition that the CO_2–N_2-13X binary system should behave in some kind of PP fashion. What

was surprising, however, is that the next two closest correlations in terms of the AREs, i.e., Cases 4 and 9, were negative in character. As just mentioned, Cases 4 and 9 would be expected to behave similarly, since they both have the highest and medium free energy sites of CO_2 respectively interracting with the lowest and highest free energy sites of N_2, hence in negative fashions. The only difference between these negative site matching manifestations is that instead

of leaving the lowest free enegy site of CO_2 unoccupied by N_2, as in Case 4, the highest free enegy site of N_2 is partitioned between the medium and lowest free enegy sites of CO_2 in Case 9, according to Eqs. 17 and 18. The perplexing question is: why did these PN (Case 4) and NUS (Case 9) site matching correlations predict almost as good as the PP correlation (Case 1) and so much better than the remaining 9 cases with very large errors in the N_2 loadings and mole

Fig. 8 Comparison of binary predictions (lines) of n–y and x–y mixed gas adsorption equilibria (symbols, Exp) for CO_2 and N_2 on 13X zeolite at $T = 45$ °C and $P = 10.1$ bar by the TPL_{CO2}–DPL_{N2} model for

Cases 1 (perfect positive, C1), 4 (perfect negative, C4) and 9 (negative unselective, C9) in Table 1

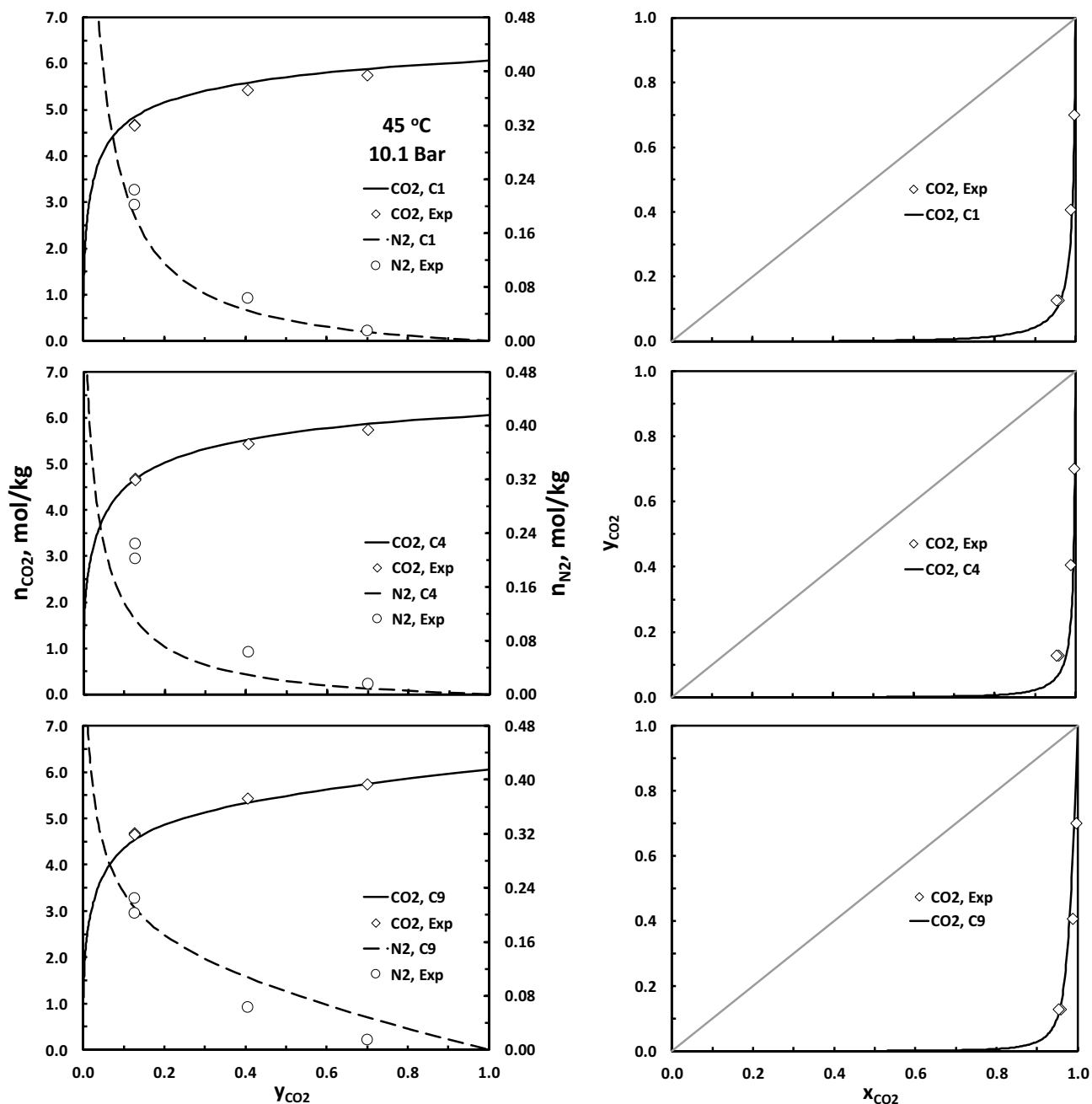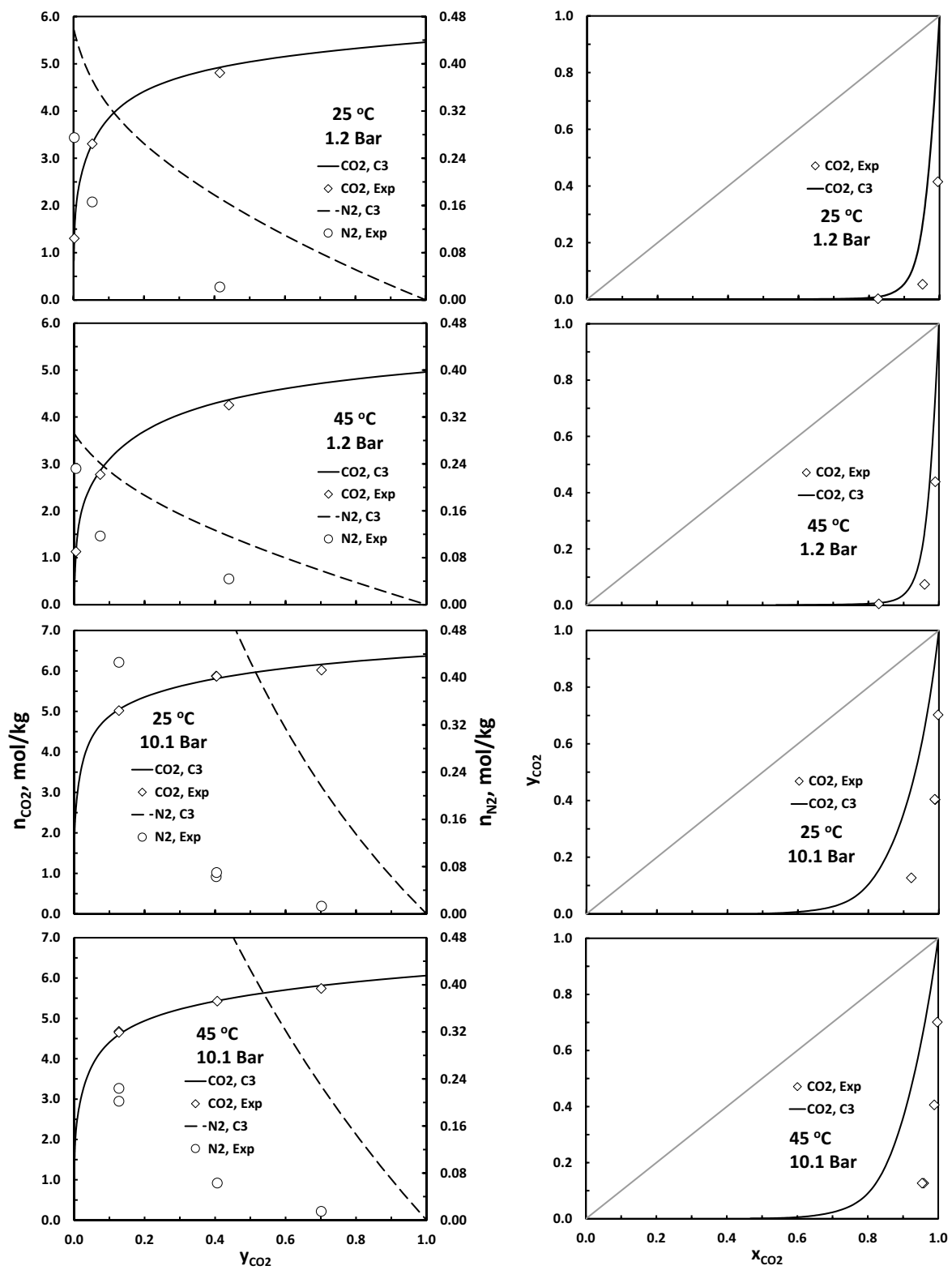**Fig. 9** Comparison of binary predictions (lines) of n–y and x–y mixed gas adsorption equilibria (symbols, Exp) for CO_2 and N_2 on 13X zeolite at $T = 25$ °C and 45 °C and $P = 1.2$ bar and 10.1 bar by the TPL_{CO2}–DPL_{N2} model for Case 3 (perfect positive, C3) in Table 1

Fig. 10 Comparison of binary predictions (lines) of *n–y* and *x–y* mixed gas adsorption equilibria (symbols, Exp) for CO_2 and N_2 on 13X zeolite at $T = 25$ °C and 45 °C and $P = 1.2$ bar by the TPL$_{CO2}$–SPL$_{N2}$ model for Cases 14 (uncorrelated, C14) and 16 (positive unselective, C16) in Table 2

fractions (Tables 4 and 5)? A plausible answer to this question became more apparent after inspecting the results from the TPL–SPL model.

3.4 TPL–SPL model predictions

There were 7 energetic site matching correlations to consider for the TPL–SPL model: one each for perfect positive (PP), uncorrelated (UC), perfect negative (PN), positive unselective (PU), and negative unselective (NU) and, two uncorrelated unselective (UCUS). For the PP, UC and PN cases, the sole N_2 site respectively occupied the highest, medium and lowest free energy sites of CO_2, in each case leaving two of the CO_2 sites unoccupied by N_2. In contrast, for the PUS and NUS cases, the sole N_2 site occupied two of the CO_2 sites in one fashion or another, with the N_2 site being split between two of the CO_2 sites according to a form of Eqs. 21 and 22, depending on the correlation, and in each case leaving one of the CO_2 sites unoccupied by N_2. For the UCUS case, the sole N_2 site occupied all three of the CO_2 sites, with the N_2 site being equally split between the three CO_2 sites according to Eqs. 17 and 18. Based on intuition and the same definitions for PP and PN as used for the TPL–DPL model, one of the positive site matching correlations, i.e., Cases 13 (PP) or 16 (PUS), was expected to provide the best predictions for this CO_2–N_2-13X binary system. The results were again quite interesting and somewhat unexpected.

Only two of the 7 cases for the TPL–SPL model exhibited similar and reasonable predictions of the experimental results for both the component loadings (Table 4) and component mole fractions (Table 5). These were Cases 14 and 16. The AREs for CO_2 were again relatively small for all 7 cases (all being less than 5% for the CO_2 loadings and less than 10% for the CO_2 mole fractions), while those for N_2 were markedly different (ranging between 41 and 826% for the N_2 loadings, and between 42 and 739% for the N_2 mole fractions). The other 5 cases completely failed in predicting both the N_2 loadings and N_2 mole fractions, with Case 15 perhaps considered as the worst correlation, based on the N_2 predictions. The disparity between the CO_2 and N_2 predictions again was not surprising and about the same as that observed with the TPL–DPL model and for the same reasons. The overall AREs from the TPL–SPL model were slightly larger compared to those from the TPL–DPL model, as might be expected.

Figure 10 compares binary predictions from the TPL–SPL model at $T = 25$ and 45 °C and $P = 1.2$ bar in terms of n–y and x–y diagrams for Cases 14 and 16, the two best cases. Figures 11 and 12 show the same information, but each at a different pressure, covering all the binary data for the CO_2–N_2-13X system [2]. Again, to exemplify how bad the predictions might become from the TPL–SPL model, Fig. 13 shows the n–y and x–y diagrams for Case 15, perhaps

the worst case of all 7 cases based on the AREs in Tables 4 and 5 for the TPL–SPL model.

In both cases in Figs. 10, 11, 12 and 13 the predictions of the x–y diagrams compared well with the experimental data, except for those in Fig. 13 at $P = 10.1$ bar. For the same reasons given earlier, the model underpredicted some of the experimental data points for N_2 to about the same extent in each case, again, tending to suggest there might be an issue with this data or lateral interactions were prevalent. Also, in both cases the predictions of the n–y diagram for CO_2 were very good, which is reflected in the relatively small AREs in Table 4. This was not the situation for the n–y diagram for N_2, where the deviations between experiment and model were much more pronounced, especially for the highest pressure in Fig. 12. Case 16, the best case according to the AREs in Tables 4 and 5, exhibited slightly smaller deviations between experiment and model for N_2 compared to Case 14. The fact that the deviations exhibited by Cases 14 and 16 were similar to each other was perhaps due to their energetic site matching correlations being similar (Table 2).

Figure 13 compares experiment with TPL–SPL model predictions at two different pressures and temperatures for the worst Case 15. Just like for the worst Case 3 of the TPL–DPL model, the x–y diagrams were also strikingly overpredicted by this model, as were the n–y diagrams for N_2 to the point where the model was not even close to reality. The model predictions of the n–y diagrams for CO_2 for this Case 15 were very good. This was true for all 7 cases, irrespective of the site matching corrleation, as was the case for all 12 TPL–DPL model cases.

Case 16 resulted in the smallest ARE overall, which was quite surprising, because, at first, it was thought that this was not in agreement with the supposition that the CO_2–N_2-13X binary system should behave in some kind of positive site matching fashion. However, after closer inspection of these TPL–SPL model results, it became clear that as long as N_2 did not occupy the lowest free energy site of CO_2, the predictions were all reasonably good. For example, Cases 13, 14 and 16 were the only three correlations of the 7 where N_2 does not interact with the lowest free energy site of CO_2 and they all had reasonable predictions, even the PP Case 13. This indicated that these three cases are similar in that they all exhibit some kind of positive site matching character. In contrast, Cases 15, 17, 18 and 19 all have N_2 interacting with the lowest free energy site of CO_2, and the corresponding predictions were very poor, especially for N_2. Although it was not as obvious for the TPL–DPL model, the same was true for all the correlations that have N_2 interacting with the lowest free energy site of CO_2, even Case 9. Thus, it was not too surprising that Case 9 had the worst predictions of the
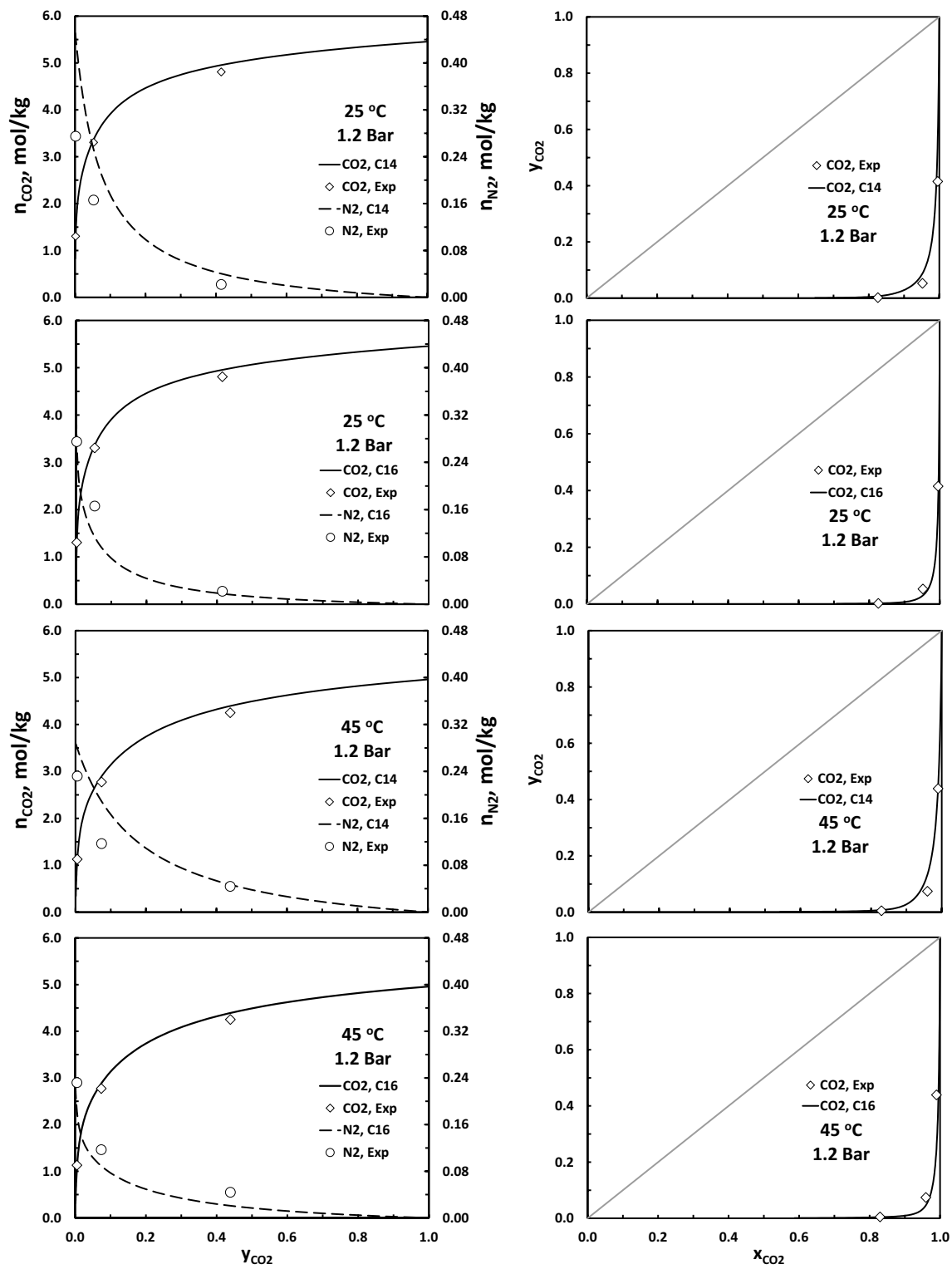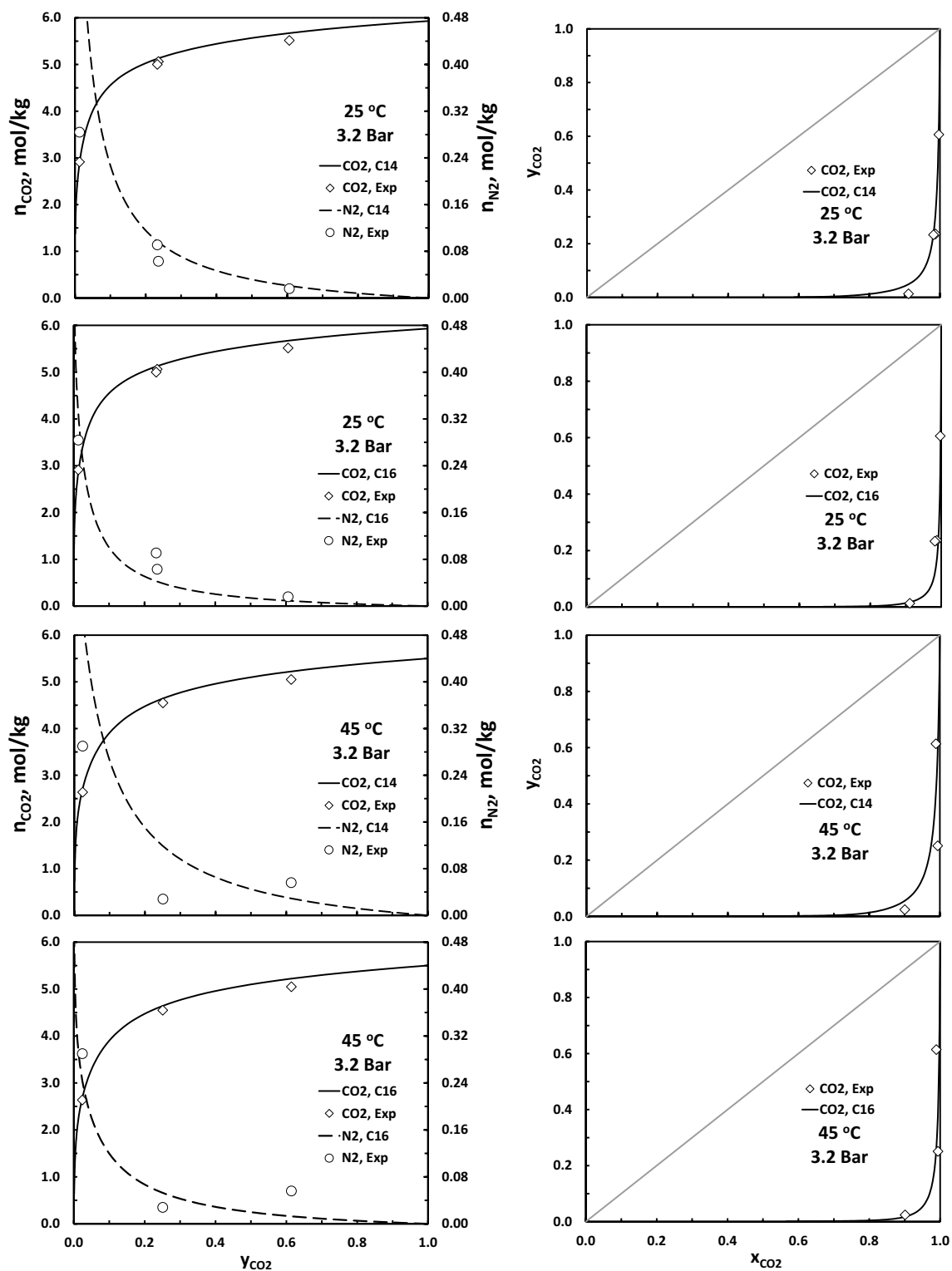
Fig. 11 Comparison of binary predictions (lines) of n–y and x–y mixed gas adsorption equilibria (symbols, Exp) for CO_2 and N_2 on 13X zeolite at $T = 25$ °C and 45 °C and $P = 3.2$ bar by the TPL$_{CO2}$–SPL$_{N2}$ model for Cases 14 (uncorrelated, C14) and 16 (positive unselective, C16) in Table 2

three best cases for the TPL–DPL model, i.e., Cases 1, 4 and 9.

4 Discussion

Overall, it was found that N_2 did not like to interact with the lowest free energy site of CO_2, but it did like to interact with both of the higher free energy sites of CO_2, not just *Site 1*. This was an interesting result, as it conceivably revealed the two known Na ion sites within the cavity of the unit cell of 13X, i.e., sites II and III, perhaps with different interaction energies, that are accessible for interaction with the quadrupoles of N_2 and CO_2. It was also clear from these results that when N_2 interacted with the lowest energy site of CO_2 too much N_2 adsorbed due to the lack of competition with CO_2 on that site. This caused both models to severely overpredict the N_2 loadings compared to experiment. Nevertheless, intuition prevailed for both the TPL–DPL and TPL–SPL models, with N_2 preferring the two higher free energy sites of CO_2 because they both have quadrupole moments.

For this CO_2–N_2-13X system, instinct suggested Case 1 would be the best correlation. This turned out to be correct, as it was the best correlation of all 19 permutations associated with the TPL–DPL and TPL–SPL models. If intuition or the suggestions provided herein are not followed, e.g., by allowing the sites to be assigned randomly, erroneous results might be obtained like for Case 3 with the TPL–DPL model and Case 15 with the TPL–SPL model.

A final note worth mentioning is that this work only considered a binary system. This was done purposely to introduce the intricacy associated with using these TPL–DPL and TPL–SPL models that must be taken seriously to ensure erroneous results are not obtained when predicting binary gas adsorption equilbria. The extension of these two models to a ternary system is even more confounding and thus challenging. Consider, for example, how to establish the energetic site matching rules for a ternary system where the single gas isotherms of each component are strictly fitted well by the TPL, DPL and SPL models. The rules would be similar to but subtly different than those established for the DPL–DPL multicomponent model [7]. This work is in progress and will be the topic of a future paper.

5 Conclusions

Two scenarios were investigated for predicting mixed gas adsorption equilibria of a binary system when the single gas isotherms of one of the components is described by the three process Langmuir (TPL) model and the single gas isotherms of the other component is described by either the dual process Langmuir (DPL) or single process Langmuir (SPL) model. For the TPL–DPL binary mixed gas model, 12 different correlations or permutations of energetic site matching exist: three perfect positive (PP), three perfect negative (PN), two positive unselective (PUS), two negative unselective (NUS) and two uncorrelated unselective (UCUS). For the TPL–SPL binary mixed gas model, 7 permutations exist: one each for PP, uncorrelated (UC), PN, PUS and NUS, and two UCUS.

For these more complex TPL–DPL and TPL–SPL systems, PP means the free energies of the various sites of the two components align in some way from high to low, while PN means they misalign in some way with high free energy sites for one component aligning with low free energy sites for the other component. PUS and NUS mean the free energies correlate in some way with the free energy of the site of one of the components distributed among two or more sites of the other component, and UCUS means the free energies do not correlate but still with some site distribution, and UC simply means the free energies of the two components on the various sites do not correlate in any meaningful way.

A consistent set of single and binary isotherms for CO_2 and N_2 on 13X zeolite were used to explore all 19 energetic site matching possibilities, with CO_2 fitted well only to the TPL single gas model and N_2 fitted equally well to either the DPL or SPL single gas model. Only three of the 12 cases for the TPL–DPL model and two of the 7 cases for the TPL–SPL model exhibited similar and reasonable predictions of the experimental results for both the component loadings and component mole fractions. The other 9 cases for the TPL–DPL model and 5 cases for the TPL–SPL model completely failed in predicting both the N_2 loadings and N_2 mole fractions. The predictions of the n–y and x–y diagrams for CO_2 for both models were all very good for all 19 cases irrespective of the site matching corrleation. This was because N_2 does not affect the adsorption of CO_2 on 13X; but, CO_2 does affect the adsorption of N_2 on 13X. So, for both models, some of the predictions of the x–y and n–y diagrams for N_2 were so strikingly poor and overpredicted, the predictions were not even close to reality. It was determined that when N_2 interacted with the lowest energy site of CO_2 too much N_2 adsorbed due to the lack of competition with CO_2 on that site. These erroneous results could happen if the wrong correlation is inadvertently chosen or if the practice of energetic site matching is unintentionally ignored and the sites are assigned randomly.

For this CO_2–N_2-13X binary system, intuition suggested for energetic site matching that PP implied the higher free enegy sites of CO_2 would align with the higher free enegy sites of N_2, because they both have quadrupole moments that interact with the Na ions in the 13X. So, it was anticipated that one of the PP site matching correlations of the 19 permutations of both models would provide the best predictions for this CO_2–N_2-13X binary system. This was indeed the
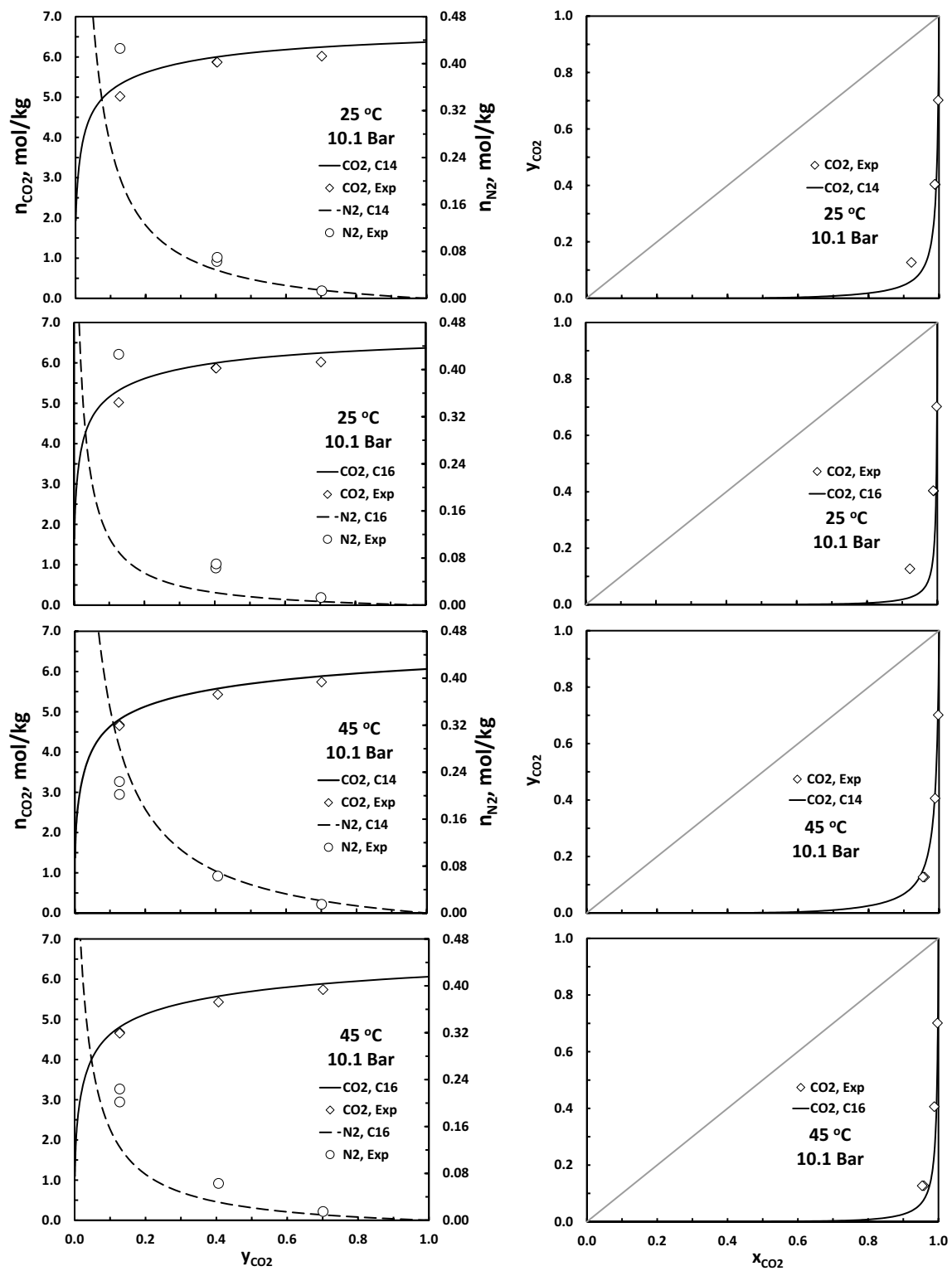
Fig. 12 Comparison of binary predictions (lines) of *n–y* and *x–y* mixed gas adsorption equilibria (symbols, Exp) for CO_2 and N_2 on 13X zeolite at $T = 25$ °C and 45 °C and $P = 10.1$ bar by the

TPL$_{CO2}$–SPL$_{N2}$ model for Cases 14 (uncorrelated, C14) and 16 (positive unselective, C16) in Table 2
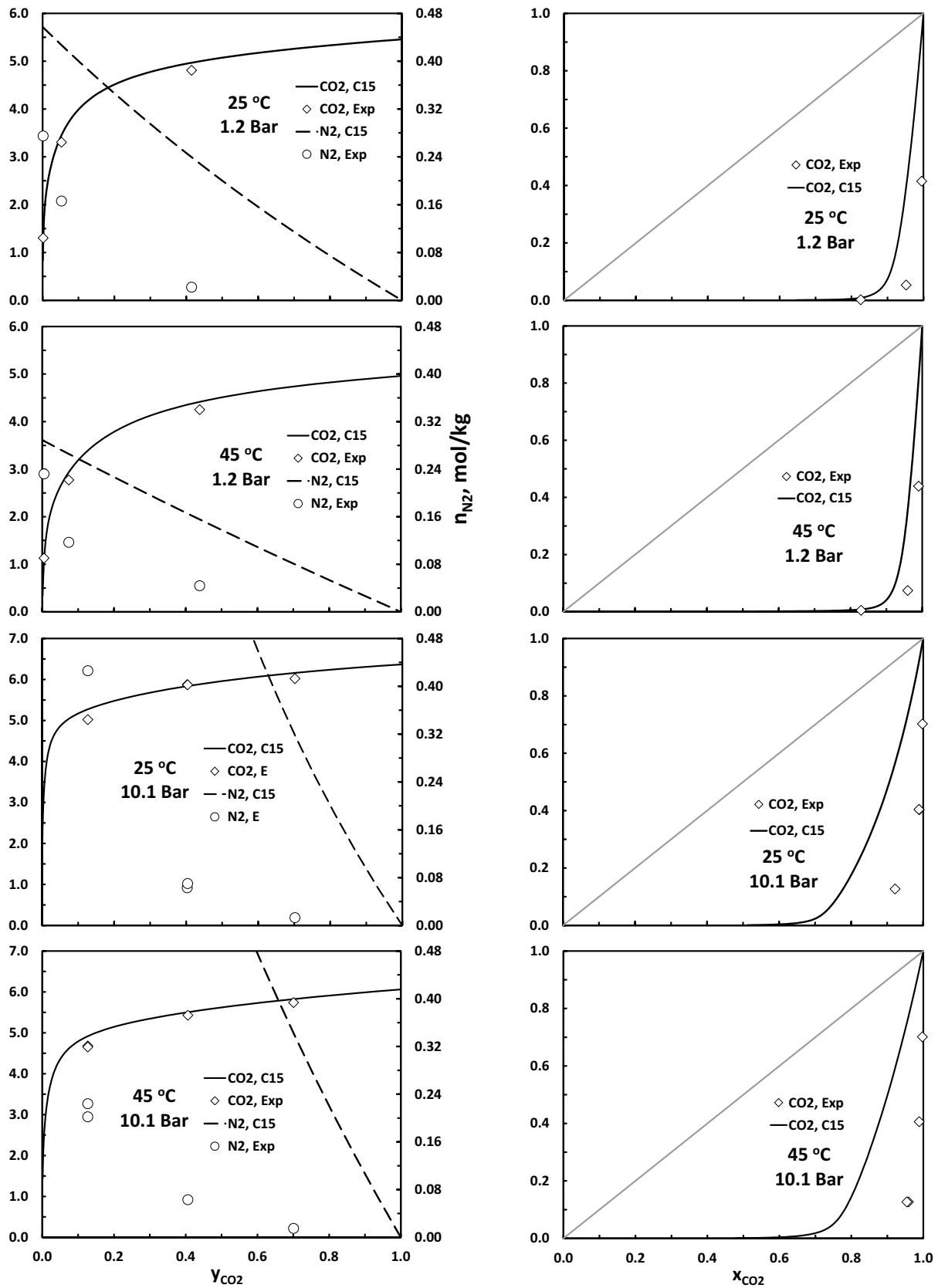
Fig. 13 Comparison of binary predictions (lines) of *n*–*y* and *x*–*y* mixed gas adsorption equilibria (symbols, Exp) for CO_2 and N_2 on 13X zeolite at $T = 25$ °C and 45 °C and $P = 1.2$ bar and 10.1 bar by the TPL_{CO2}–SPL_{N2} model for Case 15 (perfect negative, C15) in Table 2

case, with the high and low free energy sites of N_2 decidedly interacting with the high and medium free energy sites of CO_2 in a PP fashion with the low free energy site of CO_2 unoccupied by N_2. Determining that N_2 had an affinity for both of the higher free energy sites of CO_2, not just *Site 1*, was an interesting result, as it suggested 13X possibly has two different Na ion sites within its crystal structure that are energetically favorable for interaction with the quadrupoles of N_2 and CO_2.

The take home message from this analysis is simple: to properly use the single gas MPL model to predict mixed gas adsorption equilibria using one of these more complex varients, intuition about adsorbate–adsorbent interactions must be considered for each component in the gas mixture. Then, the free energies for each component on each site must be assigned, accordingly. The simpler site matching correlations appeared to be the ones to consider, for the ones with sites of N_2 distributed over two or more sites of CO_2 did not fare well. If energetic site matching is inadvertently ignored or just not applied, erroneous predictions could be obtained because the adsorption free energies for each component on each site are not properly matched or alligned.

Declarations

Conflict of interest The authors declare they have no conflicts of interest.

References

1. Cerofolini, G.F., Rudzinski, W.: Theoretical principles of single- and mixed-gas adsorption equilibria on heterogeneous solid surfaces. Stud. Surf. Sci. Catal. **104**, 1–103 (1997)
2. Hefti, M., Marx, D., Joss, L., Mazzotti, M.: Adsorption equilibrium of binary mixtures of carbon dioxide and nitrogen on zeolites ZSM-5 and 13X. Microporous Mesoporous Mater. **215**, 215–228 (2015)
3. Langmuir, I.: The adsorption of gases on plane surfaces of glass, mica and platinum. J. Am. Chem. Soc. **40**, 1361–1403 (1918)
4. Mohammadi, N., Adegunju, S.A., Erden, L., Rahman, A., Ebner, A.D., Ritter, J.A.: Adsorption equilibrium of nitrogen, oxygen, argon, carbon dioxide, carbon monoxide, methane, ethane, propane, ethylene and propylene on 13X zeolite. Unpublished Results, USC (2020)
5. Moon, H., Tien, C.: Adsorption of gas mixtures on adsorbents with heterogeneous surfaces. Chem. Eng. Sci. **43**, 2967–2908 (1988)
6. Myers, A.L.: Activity coefficients of mixtures adsorbed on heterogeneous surfaces. AIChE J. **29**, 691–693 (1983)
7. Ritter, J.A., Bhadra, S.J., Ebner, A.D.: On the use of the dual process Langmuir model for correlating unary and predicitng mixed gas adsorption equilibria. Langmuir **27**, 4700–4712 (2011)
8. Ritter, J.A., Bumiller, K.C., Tynan, K.J., Ebner, A.D.: On the use of the dual process Langmuir model for binary gas mixture components that exhibit single process or linear isotherms. Adsorption **25**, 1511–1523 (2019)
9. Talu, O., Li, J., Kumar, R., Mathias, P.M., Moyer, J.D., Jr., Schork, J.M.: Measurement and correlation of oxygen/nitrogen/5A-zeolite adsorption equilibria for air separation. Gas Sep. Purif. **10**, 149–159 (1996)
10. Valenzuela, D.P., Myers, A.L., Talu, O., Zwiebel, I.: Adsorption of gas mixtures: effect of energetic heterogeneity. AIChE J. **34**, 397–402 (1988)
11. Yang, R.T.: Adsorbents: Fundamentals and Applications. Wiley, Hoboken (2003)